UDK 678.744.32:546.284-31 ISSN 1580-2949
Original scientific article/Izvirni znanstveni članek MTAEC9, 58(2)231(2024)

# EFFICIENT PRODUCTION OF SMALL-SIZED $SiO_2$ NANOPARTICLES AND THEIR APPLICATION IN A WATERBORNE ACRYLIC-AMINO VARNISH

## UČINKOVITA IZDELAVA NANODELCEV $SiO_2$ IN NJIHOVA UPORABA ZA AMINO-AKRILNE LAKE NA VODNI OSNOVI

**Jinping Wu[1,2], Jinxiang Mao[1], Hong Liu[1], Xichuan Cao[1], Minmin Chen[2*]**
[1]School of Materials and Physics, China University of Mining and Technology, Xuzhou 221116, P. R. China
[2]School of Stomatology, Xuzhou Medical University, Xuzhou 221004, P. R. China

*Prejem rokopisa – received: 2023-00-08; sprejem za objavo – accepted for publication: 2024-02-28*

doi:10.17222/mit.2023.905

In this study, we optimized the preparation of 100–160 nm monodispersed $SiO_2$ nanoparticles and, through doping, investigated their effects on the physical properties of a water-based acrylic-amino varnish. First, using a non-fixed point feeding technique based on the half-batch sol-gel method, we enhanced the yield of small-sized monodispersed $SiO_2$ nanoparticles. To reduce the cost of production and organic-matter pollution, we assessed certain solution parameters including tetraethyl orthosilicate (TEOS), ethanol (ETOH) and ammonia in a single-reaction system. We found that the gloss, clarity, hardness, adhesion, and other physical properties of the acrylic-amino varnish were successfully enhanced through an addition of 1.2 % $SiO_2$ nanoparticles.

Keywords: $SiO_2$ nanoparticles, non-fixed point feeding, acrylic-amino varnish, physical properties

V članku avtorji opisujejo študijo optimizirane priprave enakomerno dispergiranih nanodelcev $SiO_2$ velikih od 100 do160 nm, ki naj bi se uporabljali kot dodatek amino-akrilnim lakom na vodni osnovi. Ugotavljali so učinek dodatka različne količine izdelanih nanodelcev $SiO_2$ na fizikalne lastnosti kompozita. Uporabili so tehniko polnjenja z nefiksirano točko, temelječo na pilotni sol-gel metodi. Na ta način so učinkovito izdelali manjšo količino enakomerno dispergiranih nanodelcev $SiO_2$. Da bi zmanjšali stroške izdelave in onesnaženje z organskimi snovmi so ocenili dejanske parametre raztopine, vključno s tetraetil ortosilikatom (TEOS), etanolom (ETOH) in amonijakom v enojnem reaktorskem sistemu. Ugotovili so, da so se sijaj, čistost, trdota, adhezija in druge fizikalne lastnosti kompozitnega amino-akrilnega laka močno izboljšale z dodatkom 1,2 % $SiO_2$ nanodelcev.

Ključne besede: nanodelci $SiO_2$, nefiksirana točka polnjenja, amino-akrilni lak na vodni osnovi, fizikalne lastnosti

## 1 INTRODUCTION

Small-sized $SiO_2$ nanoparticles in a range of 100–160 nm have attracted significant attention due to their small particle size, high specific surface area, large surface adsorption capacity, good dispersion and facile surface functionalization. These $SiO_2$ nanoparticles have broad applications in various fields, such as catalysis,[1,2] packaging materials,[3] coating,[4] textiles[5] and energy batteries.[6] With an increasing demand for small $SiO_2$ nanoparticles, an economical production method is increasingly required to ensure a uniform particle size and good monodispersity. So far, the sol-gel method has been considered to be a simple and efficient method for preparing $SiO_2$ nanoparticles.[7–9] Numerous studies have been conducted to investigate the key factors such as reactants, reaction time and temperature, primarily aimed at controlling the size of $SiO_2$ nanoparticles.[10–12] However, these investigations have predominantly overlooked critical aspects such as resource utilization, overall yield and environmental considerations within the reaction system.[13–17] These factors are typically influenced by the amount of tetraethyl orthosilicate (TEOS) and ethanol (ETOH) present within the reaction system. Pertinent literature indicates that for the preparation of reaction systems yielding particles in the size range of 100–160 nm, the volume ratio of TEOS to ETOH is often lower than 1/9,[10–17] and in certain cases, it can be as low as 1/43.[6] This observation highlights the inherently extensive nature of the reaction system with a high ethanol volume and the correspondingly low yield. This system is inherently unsuitable for a large-scale production, given its inherent limitations, and has the potential to result in substantial wastage of valuable resources and significant organic pollution. Therefore, to facilitate a large-scale production of $SiO_2$ nanoparticles, a comprehensive evaluation and improvement plan will be devised, focusing on two primary issues: enhancing the production efficiency and minimizing the reliance on organic solvents.

In recent years, $SiO_2$ nanoparticles have been increasingly used in the field of coatings, mainly through the use of covalent bonds, hydrogen bonds or van der Waals forces to closely combine organic and inorganic components, as these complement each other to enhance the

---

*Corresponding author's e-mail:
minminchen@xzhmu.edu.cn (Minmin Chen)

different properties of waterborne coatings.[18–21] The particle size of $SiO_2$ nanoparticles varies according to the requirements as different particle sizes lead to differences in the steric effect, optical properties, suspension state and other properties. As the outermost layer of color paint, varnish is expected to meet high technical requirements regarding the properties such as appearance, hardness and adhesion. Currently, a two-component varnish composed of acrylic resin and amino resin is not considered a mature technical direction,[22,23] and achieving the same performance and appearance of solvent-based coatings under the same construction conditions remains a challenge. Therefore, it is essential to modify waterborne varnishes. Unlike other color paint modification techniques, the materials used for a varnish modification should not affect the glossiness and transparency, as this can cause a color difference between the primer and varnish. Small-sized $SiO_2$ nanoparticles can also act as natural UV absorbers with high hardness, stability and size effects, potentially enhancing different properties of a waterborne varnish.

In this study, we successfully doubled the production and reduced the cost of a single-reaction system for the preparation of small-sized $SiO_2$ nanoparticles using a technique based on the half-batch sol-gel method.[24] This was achieved by adjusting the reaction parameters (tetraethyl orthosilicate (TEOS), ETOH and ammonia) using innovative non-fixed feeding methods. Our findings provide potential solutions for addressing the issues of a high solvent consumption, low resource utilization rates and low yield associated with conventional sol-gel methods. Furthermore, we studied the effects of different $SiO_2$ nanoparticle concentrations on the physical properties of a waterborne acrylic-amino varnish through doping, which promoted the development of water-based coatings and reduced environmental pollution.

## 2 MATERIALS AND METHODS

### *2.1 Materials*

TEOS, ammonia and ETOH were purchased from Sinopharm Chemical Reagent (China) while deionized water was produced using an EPED-E2-20TJ water purification system. Melamine formaldehyde resin, a wetting agent, and a leveling agent (Bike Chemical) were obtained from Shanghai Kaiin Chemical Co. (China). Acrylic resin was obtained from Xingtai Fuyu New Materials Co. (China), ethylene glycol butyrate was procured from Shanghai Jiushi Chemical Co. (China), and dipropylene glycol methyl ether was obtained from Guangzhou Honghai Chemical Co. (China). The rheological agent (299) was procured from Shanghai Guangbai New Materials Co. (China), and dimethylethanolamine was obtained from BASF Co. (Germany). The substrate consisted of a 120 × 50 × 0.28 cm tinplate plate, which was purchased from Guangzhou Desmanyi Instrument Co. (China).

### *2.2 Preparation of $SiO_2$ nanoparticles*

**Figure 1** illustrates the preparation of $SiO_2$ nanoparticles with non-fixed point feeding based on the half-batch sol-gel method. TEOS was first dissolved in an ETOH solution. Subsequently, deionized water, ETOH and ammonia were mixed evenly with magnetic stirring. The TEOS-ETOH solution was carefully drippled onto the bottom of the reaction solution at four points, covering the first and second feeding locations, within 2 min.

The specific preparation schemes employed the non-fixed point feeding approach (**Figure 1**), with detailed specifications described as follows. Scheme 1 aimed to adjust the volumes of TEOS to the maximum capacity of the single-reaction system. First, 90 mL ETOH, 40 mL deionized water, and 5 mL ammonia were

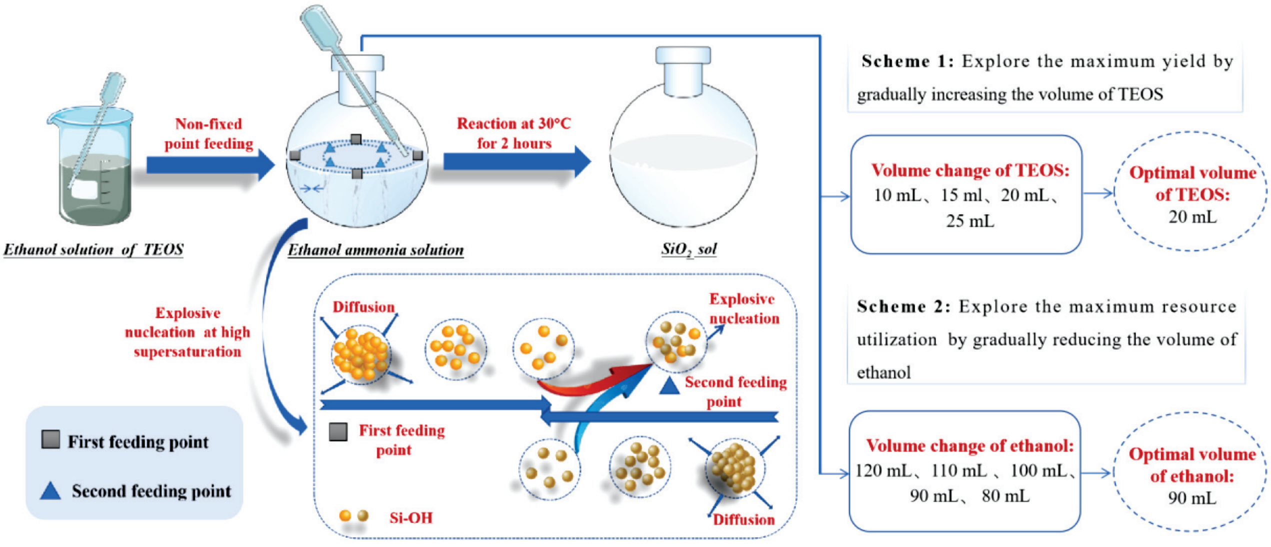

**Figure 1:** Schematic of the $SiO_2$ nanoparticle preparation with non-fixed point feeding

stirred at 30 °C for 15 min. Then different volumes of TEOS (10, 15, 20 and 25) mL and 30 mL ETOH were fully mixed and quickly added to the above solution for 2 h. Scheme 2 minimized the production costs of the single-reaction system by reducing ETOH and fine-tuning the volume of ammonia. The ETOH solvent was replaced with water while keeping the total volume constant, using a fixed amount of 20 mL of TEOS. The volumes of deionized water, ETOH and ammonia were varied between 50–80 mL, 110–80 mL and 5–3 mL, respectively. The preparation process was the same as for Scheme 1. The prepared mixture was centrifugally collected by ETOH and water alternately. The obtained samples were labeled as $S_N(T/E)$ where $N$ represents the volume of ammonia, and $T/E$ is the volume ratio of TEOS to ETOH.

### 2.3 Preparation of the coating samples

The prepared and undried $SiO_2$ nanoparticles were dispersed in water through high-speed stirring and ultrasonication to form a $SiO_2$ sol with a certain concentration. Next, 50 % acrylic resin, 2.5 % dimethylethanolamine and 6 % cosolvent were completely stirred and neutralized in a container equipped with a stirring device. At 700 $min^{-1}$, we added 10 % melamine formaldehyde resin, 5 % dipropylene glycol methyl ether and 2 % ethylene glycol monobutyl ether, and the mixture was stirred for 10 min. Then, the $SiO_2$ nanoparticle sol with different mass percentages of (0.3, 0.6, 0.9, 1.2, 1.5 and 1.8) % was slowly added while stirring the mixture at 1100 $min^{-1}$ for 15 min. Finally, the 0.2 % wetting agent and 0.2 % leveling agent were added at 700 $min^{-1}$ and stirred for 10 min to obtain a $SiO_2$ nanoparticle composite acrylic-amino varnish emulsion. The prepared emulsions were sprayed on a carbon steel surface, which was pre-treated with sandpaper. The thickness of the film was 0.26 ± 0.05 mm. After leveling for 5 min, the samples were transferred to an oven at 140 °C and baked for 15 min.

### 2.4 Characterization and measurements

The surface morphologies of $SiO_2$ nanoparticles were assessed using a JSM-6700F field-emission scanning electron microscope (FE-SEM) with an accelerating voltage of 10.0 kV. The size and monodispersity of $SiO_2$ nanoparticles were characterized through dynamic light scattering (DLS, NanoBrook Omni, Brookhaven Instruments). The optical absorbance values were determined in a wavelength range of 190–1100 nm using a UV-Vis spectrophotometer (Evolution 300, Thermo). The gloss values of the coating films were measured using a gloss meter instrument (3 nh gloss meter, Shenzhen Sanenshi Technology Co., China), according to the GB 1743-1979 standard under the 60° measurement mode. On each sample, at least five different points were measured, and the average values were reported. The static water contact angle of the coating film surface was measured using a contact angle measurement instrument (Shanghai Zhongchen Digital Technology Equipment Co., China). A pencil hardness test was performed according to the GB/T 6739-2006 standard, and an Elcometer 510 automatic pull-out adhesion tester was used for the adhesion test according to the GB/T 5210-2006 standard.

## 3 RASULTS AND DISCUSSION

According to Scheme 1, by fixing the ETOH, water and ammonia volumes in the reaction solution, the influence of the TEOS volume on the particle size and morphology of the nanoparticles was studied. For the experiments with (10, 15 and 20) mL of the TEOS solution, the average size of the prepared particles was (120, 135 and 156) nm, respectively, and the variation range of the particle size was within 30 nm (**Figure 2a** to **2c**). The polymer dispersity index (PDI) varied between 0.039–0.192, indicating an excellent monodispersity of the nanoparticles. Using the non-fixed point feeding method (**Figure 1**), the high-concentration –Si–O– chains or silanol groups resulting from the hydrolysis of TEOS un-

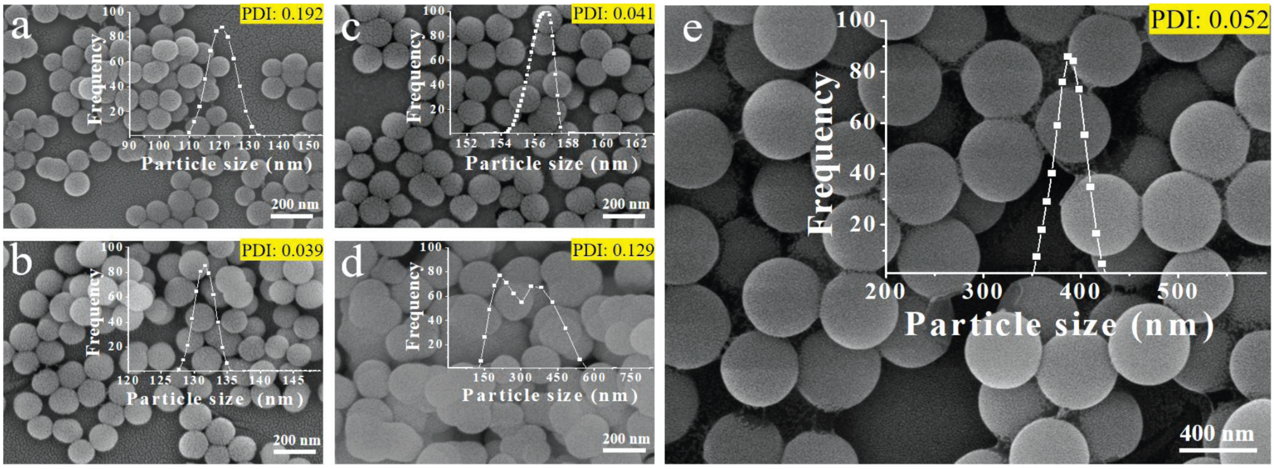

**Figure 2:** SEM and DLS images of the $SiO_2$ nanoparticles with different TEOS volumes: a) $S_5(10/120)$, b) $S_5(15/120)$, c) $S_5(20/120)$, d) $S_5(25/120)$, e) $S_5(20/120)$ in the fixed feeding point

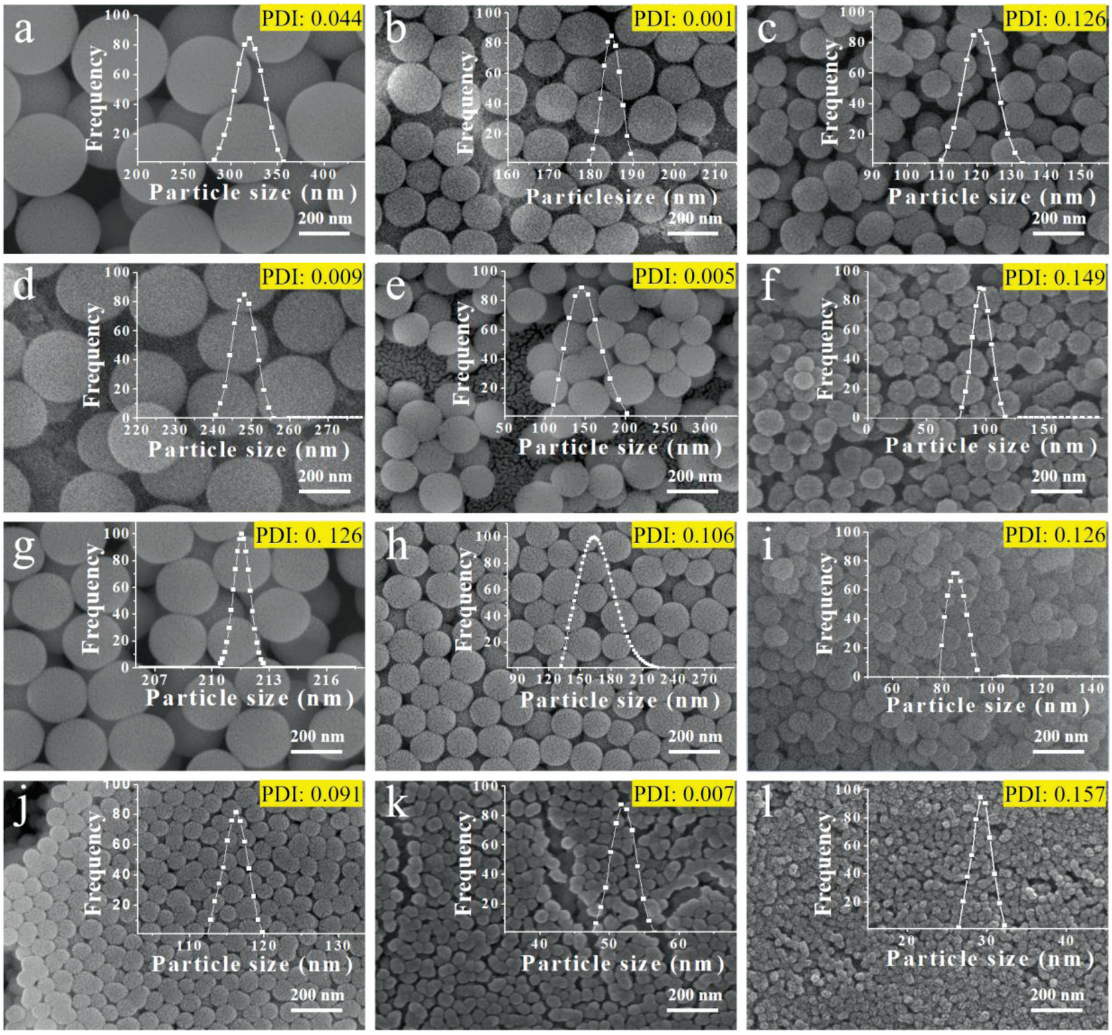

**Figure 3:** SEM and DLS images of the $SiO_2$ nanoparticles prepared with different ETOH volumes: a) $S_5$(20/110), b) $S_4$(20/110), c) $S_3$(20/110), d) $S_5$(20/100), e) $S_4$(20/100), f) $S_3$(20/100), g) $S_5$(20/90), h) $S_4$(20/90), i) $S_3$(20/90), j) $S_5$(20/80), k) $S_4$(20/80) and l) $S_3$(20/80)

derwent supersaturation and nucleated within a certain range of the feeding point, while the other free active groups became diffused. With an increasing TEOS concentration, the difference in the active group concentration between the feeding points and their surroundings increased. The accelerated diffusion led to a faster supersaturation between the feeding points, thus increasing the nucleation. Consequently, the average particle size of the particles obtained with non-fixed point feeding remained relatively constant and was much smaller than that obtained with fixed point feeding (**Figure 2c** and **2e**). Moreover, the increase in TEOS improved the yield of small-sized $SiO_2$. Further increase in the TEOS volume to 25 mL (**Figure 2d**) prompted the particle agglomeration, which may be due to the close contacts between particles, dehydration and condensation of surface hydroxyl groups.

Scheme 1 optimized the TEOS amount in the single-reaction system. However, ETOH, as an organic solvent, accounted for the largest proportion in the reaction system, which may cause organic matter pollution and waste of resources. To solve this issue, in Scheme 2, ETOH was replaced with water while keeping the total volume constant at a fixed volume of 20 mL of TEOS. When the amount of ETOH is reduced to 110 mL for $S_5$(20/110) (**Figure 3a**), the nanoparticle average diameter increases to 320 nm in comparison to $S_5$(20/120) (**Figure 2c**). The increase in the nanoparticle size is ascribed to the increased water that accelerated hydrolysis and condensation of the active group, crystal nucleation and growth. ETOH is gradually reduced, resulting in a successive decrease in the particle size (**Figures 3d, 3g** and **3j**). The reduction of ethanol, the dissolvent of TEOS, reduces the hydrolysis rate of TEOS, resulting in smaller size nanoparticles. Although **Figure 3j** shows an average small size of 116 nm, both the yield and productivity are low (**Figure 4b**). Therefore, to obtain small-sized nanoparticles with high yield and productivity, the ammonia volume is slightly adjusted. Then, small-sized nanoparticles (100–160 nm) with high monodispersity (a PDI of 0.005–0.126) are prepared (as shown in **Figures 3c, 3e** and **3h**).

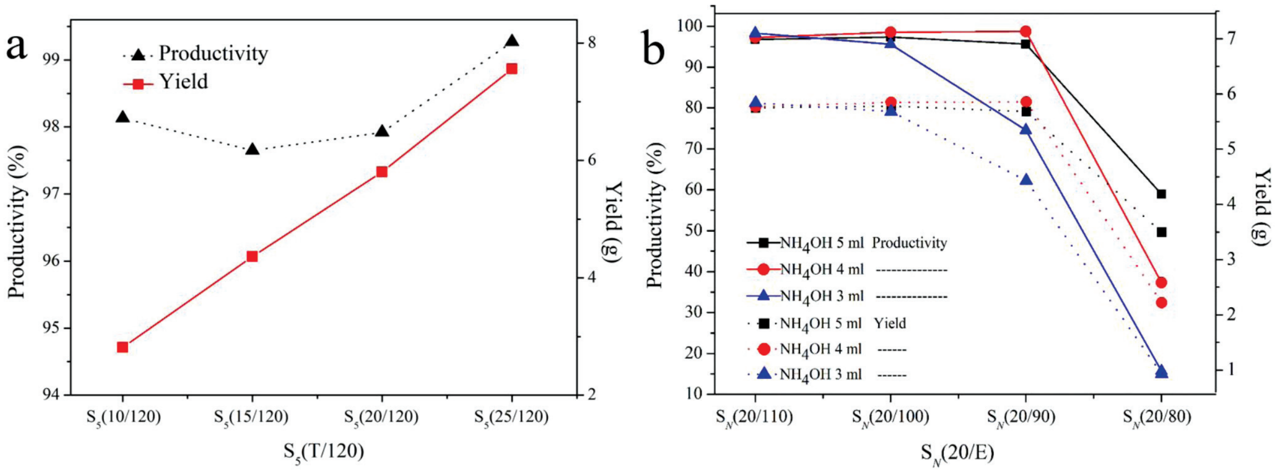

**Figure 4:** Relationship between the productivity and yield of SiO$_2$ nanoparticles, in accordance with the TEOS/ETOH volume ratio ($V_T/V_E$): a) $S_5(T/120)$ and b) $S_N(20/E)$

**Table 1:** Required $V_T/V_E$ ratio and ETOH volume concentration for preparing small SiO$_2$ nanoparticles

| Samples | $S_5$(10/120) | $S_5$(15/120) | $S_5$(20/120) | $S_3$(20/110) | $S_4$(20/100) | $S_4$(20/90) |
|---|---|---|---|---|---|---|
| $d$ (nm) | 125 | 130 | 156 | 120 | 145 | 150 |
| $C_v$ ($V_{ETOH}/V_{overall}$%) | 68.5% | 66.6% | 64.8% | 60.1% | 54.3% | 48.9% |
| $V_T/V_E$ ($V_{TEOS}/V_{ETOH}$) | 1/12 | 1/8 | 1/6 | 2/11 | 1/5 | 2/9 |

The parameters of small-sized monodisperse SiO$_2$ were optimized in the single-reaction system. Moreover, the yield and productivity of nanoparticles based on Scheme 1 and Scheme 2 were calculated as shown in **Figures 4a** and **4b**. According to **Figure 4a**, there was a linear increase in the yield (>97.0 %) of SiO$_2$ nanoparticles in relation to the volume of TEOS. Additionally, the production of the single system was increased by 2 times under the condition that the obtained SiO$_2$ nanoparticles were homogeneous and exhibiting a good morphology. As shown in **Figure 4b**, a productivity of more than 97.0 % was obtained for $S_N$(20/110) and $S_N$(20/100) while maintaining yield. However, there was a significant decrease in yield and productivity when the volume of ETOH was reduced to 80 mL, contributing to a challenging hydrolysis of TEOS in the limited ETOH environment.

Considering the experimental results, small nanoparticles with high productivity and monodispersity using Schemes 1 and 2 were selected for the cost calculation (**Table 1**). SiO$_2$ nanoparticles with a uniform particle size (100–160 nm) and high productivity were obtained after reducing the ETOH concentration by 19.6 %. Compared with the existing sol-gel preparation method,[24] the single-reaction system allowed a lower resource consumption and cost for producing small SiO$_2$

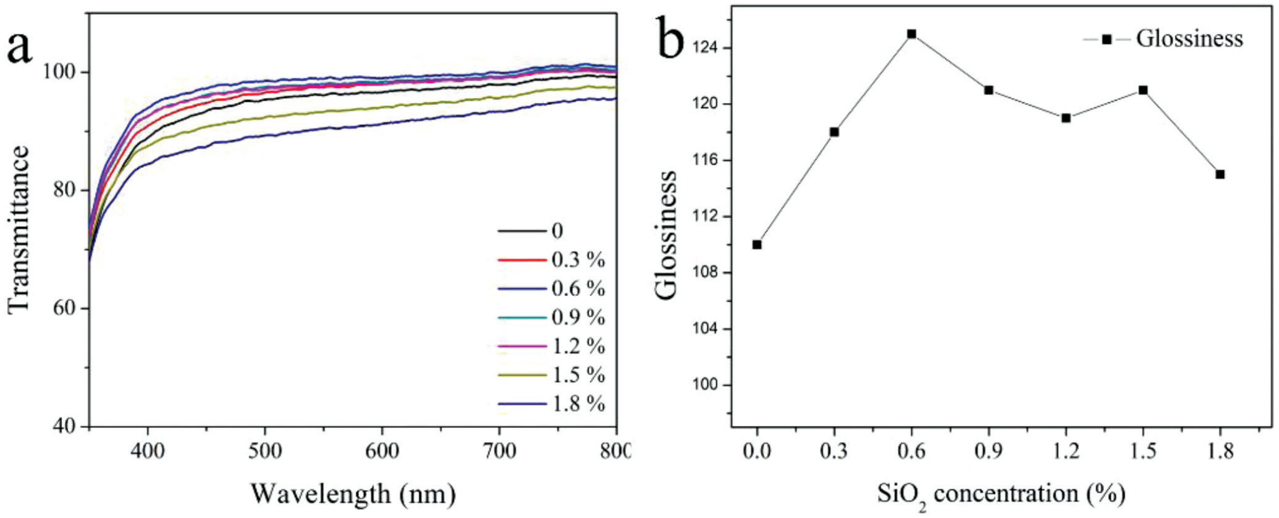

**Figure 5:** a) UV spectrophotometric test and b) gloss test of the acrylic-amino coatings containing SiO$_2$ nanoparticles with different concentrations

**Table 2:** Physical property test of the acrylic-amino coating with different $SiO_2$ nanoparticle concentrations

| Particle concentration (%) | 0 | 0.3 | 0.6 | 0.9 | 1.2 | 1.5 | 1.8 |
|---|---|---|---|---|---|---|---|
| Adhesion (MPa) | 4.65 | 4.34 | 4.69 | 5.02 | 5.41 | 4.57 | 4.46 |
| Pencil hardness (H) | 2 | 2 | 2 | 3 | 3 | 2 | 2 |
| Contact angle (°) | 90.66 | 91.25 | 92.67 | 92.33 | 92.50 | 93.60 | 93.78 |

nanoparticles. These findings pave the way for an economical and environmentally friendly mass production.

As shown in **Figure 5a**, the coating paint emulsion with a 0.3–1.2 % particle addition had higher light transmittance than the original emulsion, and the highest gloss value was 124 GU higher than that of the original paint film (**Figure 5b**). Therefore, the addition of $SiO_2$ nanoparticles did not reduce the transparency and gloss of the original varnish film. In addition, when the particle concentration was 1.2 %, the hardness and adhesion of the paint film increased to 3H and 5.41 MPa, respectively (**Table 2**). The added nanoparticles filled in the gaps created by the cross-linking of the organic molecular chains at high temperatures. However, a large number of hydroxyl groups on the surface of the particles could produce hydrogen or chemical bonds with the organic molecular chains, thus causing the paint film to be more stable and less prone to damage. In summary, $SiO_2$ nanoparticles effectively improved the physical properties of the original coating without changing its appearance.

## 4 CONCLUSIONS

In this study, we introduced a new feeding method via the semi-batch sol-gel preparation of $SiO_2$ nanoparticles. Following this feeding method, the TEOS reaction amount of the single-reaction system doubled, and the size of the obtained $SiO_2$ nanoparticles was maintained at 100–160 nm. In addition, the amount of ETOH in the reaction system was further reduced to explore efficient, green and economical synthesis solutions. Different $SiO_2$ nanoparticle concentrations were mixed into an acrylic-amino varnish emulsion and we studied the effect of the concentration on the physical properties of the varnish. The results showed that an addition of 1.2 % $SiO_2$ nanoparticles improved the UV transmittance, adhesion, hardness and gloss of the coating.

### Author contribution

**Jinping Wu:** Conceptualization, data curation, writing the original draft. **Jinxiang Mao:** Writing, reviewing and editing. **Hong Liu:** Rivising**. Xichuan Cao:** Conceptualization, methodology, investigation, supervision. **Minmin Chen:** Supervision, writing, reviewing and editing.

### Acknowledgements

This work was supported by the National Natural Science Foundation of China [grant number 22120102001] and Scientific Research Foundation for the Talents of Xuzhou Medical University [grant number D2021032].

### Declaration of no competing interest

The authors declare that they have no known competing financial interests or personal relationships that could have influenced the work reported in this paper.

### Data availability

The data that support the findings of this study are available from the corresponding authors upon reasonable request.

## 5 REFERENCES

[1] M. N. Khrizanforov, S. V. Fedorenko, A. R. Mustafina, V. V. Khrizanforova, K. V. Kholin, I. R. Nizameev, T. V. Gryaznova, V. V. Grinenko, Y. H. Budnikova, Nano-architecture of silica nanoparticles as a tool to tune both electrochemical and catalytic behavior of NiII@$SiO_2$, RSC Adv., 9 (**2019**), 22627–22635

[2] S. V. Fedorenko, M. E. Jilkin, T. V. Gryaznova, E. O. Iurko, O. D. Bochkova, A. R. Mukhametshina, I. R. Nizameev, K. V. Kholin, R. Mazzaro, V. Morandi, Silica nanospheres coated by ultrasmall $Ag^0$ nanoparticles for oxidative catalytic application, Colloids Interface Sci. Commun., 21 (**2017**), 1–5

[3] R. Zhang, X. Wang, M. Cheng, Preparation and characterization of potato starch film with various sizes of nano-$SiO_2$, Polymers, 10 (**2018**), 1172–1188

[4] A. S. Nguyen, T. D. Nguyen, T. T Thai, A. T. Trinh, G. V. Pham, H. Thai, D. L. Tran, T. X. H. To, D. T. Nguyen, Synthesis of conducting PANi/$SiO_2$ nanocomposites and their effect on electrical and mechanical properties of antistatic waterborne epoxy coating, J. Coat. Technol. Res., 17 (**2020**), 361–370

[5] N. F. Attia, M. Moussa, A. M. F. Sheta, R. Taha, H. Gamal, Synthesis of effective multifunctional textile based on silica nanoparticles, Prog. Org. Coat., 106 (**2017**), 41–49

[6] J.-X. Mao, M.-M. Chen, Y. Deng, H. Liu, Z. Ju, Z. Xing, X.-C. Cao, Synthesis of uniform silica nanospheres wrapped in nitrogen-doped carbon nanosheets with stable lithium-ion storage properties, Mater. Sci., 54 (**2019**), 12767–12781

[7] E. D. H. Mansfield, Y. Pandya, E. A. Mun, S. E. Rogers, I. Abutbul-Ionita, D. Danino, A. C. Williams, V. V. Khutoryanskiy, Structure and characterisation of hydroxyethylcellulose-silica nanoparticles, RSC Adv., 8 (**2018**), 6471–6478

[8] W. Cheng, Z. Xu, S. Chen, J. Ai, J. Lin, Q. Chen, Compatibilization behavior of double spherical TETA-$SiO_2$ŽPDVB Janus particles anchored at the phase interface of acrylic resin/epoxy resin (AR/EP) polymer blends, ACS Omega., 4 (**2019**), 17607–17614

[9] X.-Y. Sun, J.-L. Tu, L. Li, W.-N. Zhang, K. Hu, Preparation of wide-angle and abrasion-resistant multi-layer antireflective coatings by $MgF_2$ and $SiO_2$ mixed sol, Colloids Surf. A: Physicochem. Eng. Aspects, 602 (**2020**), 1–12

[10] T. M. Arantes, A. H. Pinto, E. R. Leite, E. Longo, E. R. Camargo, Synthesis and optimization of colloidal silica nanoparticles and their functionalization with methacrylic acid, Colloids Surf. A: Physicochem. Eng. Aspects, 415 (**2012**), 209–217

[11] R. J. González-Álvarez, I. Naranjo-Rodríguez, M. P. Hernández-Artiga, J. M. Palacios-Santander, L. Cubillana-Aguilera, D. Bellido-Milla, Experimental design applied to optimisation of silica nanoparticle size obtained by sonosynthesis, J. Sol-Gel Sci. Technol., 80 (**2016**), 378–388

[12] R. D. Aspasio, J. F. D. Silva, R. Borges, J. Marchi, Sol-gel synthesis of amorphous silica nanoparticles: Study of the process parameter influence on structure and particle size distribution, Mater. Sci. Forum., 912 (**2018**), 77–81

[13] M. Shekarriz, R. Khadivi, S. Taghipoor, M. Eslamian, Systematic synthesis of high surface area silica nanoparticles in the sol-gel condition by using the central composite design (CCD) method, Can. J. Chem. Eng., 92 (**2014**), 828–834

[14] G.-Y. Ren, H.-J. Su, S.-D. Wang, The combined method to synthesis silica nanoparticle by Stöber process, J. Sol-Gel Sci. Technol., 96 (**2020**), 108–120

[15] Y. Yin, R. Huang, Y. Xu, C. Wan, Preparation and characterization of highly dispersed silica nanoparticles via nonsurfactant template for fabric coating, Text. Inst., 108 (**2017**), 1662–1668

[16] S. Prabha, D. Durgalakshmi, P. Aruna, S. Ganesan, Influence of the parameters in the preparation of silica nanoparticles from biomass and chemical silica precursors towards bioimaging application, Vacuum, 160 (**2019**), 181–188

[17] R. S. Fernandes, I. M. Raimundo, M. F. Pimentel, Revising the synthesis of Stöber silica nanoparticles: A multivariate assessment study on the effects of reaction parameters on the particle size, Colloids Surf. A: Physicochem. Eng. Aspects, 577 (**2019**), 1–7

[18] R. Eslami, R. Bagheri, Y. Hashemzadeh, M. Salehi, Optical and mechanical properties of transparent acrylic based polyurethane nano Silica composite coatings, Prog. Org. Coat., 77 (**2014**), 1184–1190

[19] A. Gharieh, A. mirmohseni, M. Khorasani, Preparation of UV-opaque, Vis-transparent acrylic-silica nanocomposite coating with promising physico-mechanical properties via miniemulsion polymerization, J. Coat. Technol. Res., 16 (**2019**), 781–789

[20] G.-M. Zhao, C.-X. Ding, M.-Z. Pan, S.-C. Zhai, Fabrication of NCC-$SiO_2$ hybrid colloids and its application on waterborne poly(acrylic acid) coatings, Prog. Org. Coat., 122 (**2018**), 88–95

[21] P. Dileep, S. Jacob, S. K. Narayanankutty, Functionalized nanosilica as an antimicrobial additive for waterborne paints, Prog. Org. Coat., 142 (**2020**), 1–7

[22] C. Xiong, L. Chen, Synthesis of High Solid Content Waterborne Acrylic Resin and Preparation of its Amino Baking Paint, Shanghai Coatings, 55 (**2017**), 8–10

[23] F. Xu, Z.-Y. Zhuang, H.-Q. Zhang, B.-Y. Zhu, Z. Hu, K. Zhu, H.-G. Liu, Y.-Y. Wang, M. Liu, Y.-P. Wang, Preparation and Application of Environmental Friendly Waterborne Acrylic-Amino Baking Coatings, Coatings Technology & Abstracts, 38 (**2017**), 1–5

[24] D. Nagao, H. Nakabayashi, H. Ishii, M. Konno, A unified mechanism to quantitatively understand silica particle formation from tetraethyl orthosilicate in batch and semi-batch processes, Colloid Interface Sci., 394 (**2013**), 63–68